Hindawi
Advances in Civil Engineering
Volume 2019, Article ID 7306850, 10 pages
https://doi.org/10.1155/2019/7306850

Research Article

Influence of Different Advancing Directions on Mining Effect Caused by a Fault

Lishuai Jiang[1], **Pu Wang**[2,3], **Pengqiang Zheng**[2,3], **Hengjie Luan**[1], **and Chen Zhang**[1]

[1]*State Key Laboratory of Mining Disaster Prevention and Control Co-founded by Shandong Province and the Ministry of Science and Technology, Shandong University of Science and Technology, Qingdao 266590, China*
[2]*Department of Resources and Civil Engineering, Shandong University of Science and Technology, Tai'an 271019, China*
[3]*National Engineering Laboratory for Coalmine Backfilling Mining, Shandong University of Science and Technology, Tai'an 271019, China*

Correspondence should be addressed to Pu Wang; 15854848872@163.com

Received 15 August 2018; Revised 26 November 2018; Accepted 29 November 2018; Published 13 January 2019

Academic Editor: Marco Corradi

To study the correlation among advancing direction, strata behaviors, and rock burst induction, two physical models utilizing similar materials are established. Subsequently, the influence of advancing direction on the mining effect, caused by a fault, is studied. Moreover, the rock bursts affected by faults with different mining directions are compared and analyzed. The results show that the overlying structure varies notably, affected by fault cutting and fault dip, and the fault-affected zone and the cause of induced rock burst differ with different mining directions. However, regardless of mining directions, the overlying structure of the hanging wall is stable and fault activation is not obvious, while that of the footwall is relatively active and fault activation is violent; the risk of rock burst on the footwall is larger than that of mining on the hanging wall. Finally, an engineering case regarding two rock bursts in panel 6303 is used to verify some physical simulation results to a certain extent. Study results can serve as a reference for face layout and prevention of rock bursts under similar conditions.

1. Introduction

Because of the complicated geological conditions and stress environment of deep coal mines, the intensity and counts of rock bursts have increased notably. Recently, the number of Chinese coal mines with rock burst induction has increased dramatically, exceeding 180 and mainly distributed in Northeast and East China [1]. Herein, many of them occur near the fault, seriously threatening production safety of underground coal mines [2–4]. For instance, several rock burst accidents, which can lead to the devices being pulled down, support being pushed over, and serious damage to roadways, occurring near the fault in the Jining No. 3 coal mine, Baodian coal mine, Muchengjian coal mine, and Gucheng coal mine, have been causing serious casualties [5, 6]. Figure 1 depicts several on-site images after a rock burst accident induced by a fault in the Baodian coal mine. Hence, studying the correlation between mining operations and fault occurrence is necessary and important.

Considerable studies regarding strata behaviors or fault activation-slipping with a fault occurrence have been conducted. For instance, Ji et al. [7] studied the evolution of mining stress with a working face advancing towards a fault by numerical simulation. Jiang et al. [8, 9] studied the laws of fault activation and the induced characteristics of rock burst. Sainoki and Mitri [10] studied the fault-slipping mechanism by dynamic numerical analysis and found that fault dip angle and mining depth affected the fault-slipping notably. Wang et al. [4], Jiang et al. [11], and Jiang et al. [12] studied the strata behaviors with conditions of thick hard strata and fault and revealed the rock burst-inducing mechanism. Zhang et al. [13] explained the inducing mechanism of the rock burst caused by fault based on the stick-slip theory. Wang

(a) (b)

Figure 1: Field images of sites captured after accidents. (a) Devices being pulled down. (b) Support being pushed over.

et al. [14], Peng et al. [15], and Liu et al. [16] studied the failure process of overlying strata affected by a fault utilizing physical simulation and deduced that the fault is activated easily with a footwall face advancing towards fault. Zhang et al. [17, 18] developed a new similar solid-fluid coupling material and conducted a feasibility analysis of the simulated materials, in order to study the expansion-activation of concealed fault. Jiang et al. [6] used the field observations of microseismic energy and counts to study the relationship between fault activation and rock burst.

The aforementioned studies have either only studied the strata behavior regularity with a working face advancing towards a fault but did not continue to analyze the relationship between mining activities, fault activation-slipping, and the rock burst risk and its dangerous area in detail or only studied the fault behaviors and their effect on the rock burst but did not consider the influence of mining direction on the risk of rock burst and its regional division. In fact, as to different faults and mining directions, the overlying strata present different failure-movement characteristics during the mining process, and fault activation-instability and its inducing way to rock burst are different, resulting in the degree of dynamic pressure, the delineation of dangerous areas, and their subsequent controls being also different. Hence, it is necessary to carry out an in-depth study on mining effect in different mining directions under the influence of faults and to analyze and explain the relationship between mining effect, fault activation-instability, and rock burst induction. This can optimize the panel layout affected by the burst danger near faults and provide a basis and guidance for the follow-up work on prevention and control of dangerous areas of rock burst near the fault affected-zone.

By considering the advantages of the physical simulation test [14, 19], two physical models utilizing similar materials (i.e., river sand, calcium carbonate, and gypsum) are established in this paper; then, progressive mining operations with different advancing directions are simulated. Moreover, the influence of advancing directions on mining effect caused by a fault is studied, and the rock burst risks with different mining directions are compared and analyzed. Study results can serve as a reference for face layout and prevention of rock bursts under similar conditions.

2. Physical Simulation Test

In this paper, a physical simulation test, which is scaled a prototype in the laboratory and should obey the similarity theory, is conducted [20]. The rock properties of the physical model are based on the comprehensive geological histogram and its physical-mechanical parameters for No. 104 district in the Yangliu coal mine. Finally, two models, marked as Model 1 and Model 2, are established. Herein, Model 1 simulates a face in the footwall passing through a fault, while Model 2 simulates a face in the hanging wall passing through a fault. In addition, the two models have the same parameters: a fault dip angle of 50°, fault fall height of 4 m, and coal seam mining thickness of 8 m.

Table 1 lists the similarity ratios between the prototype and physical model, by referring to the calculation method in the previous studies [14, 21–23]. The specific calculation method has the following parameters: $C_l = l_m/l_p = 1/200$, $C_\rho = \rho_m/\rho_r = 1/1.5$, C_σ (C_E) $= C_l C_\rho = 1/300$, and $C_t = C_l^{1/2} = 14$. The test bed with the dimension of 3000 mm (length) × 400 mm (width) × 1800 mm (height) is chosen. A total iron quantity of 500 kg positioned on top of the physical models is determined to present the failed simulated strata. Moreover, considering the performance characteristics and economic practicality of similar materials, river sand, gypsum, and calcium carbonate are chosen, and uniaxial compression tests are conducted to determine the materials ratio, as listed in Table 2.

The stress-displacement monitoring system is presented as follows: an Electronic Total Station and reflectors are used to depict the displacement characteristic, and the DH3815N stress-strain testing system and sensors (totally using 35 of Model 1 and 38 of Model 2) are installed to present the stress characteristic. The layout of displacement and stress monitoring points is being realized by considering reference [14].

Finally, the overview of two physical models and their monitoring devices is shown in Figure 2. It should be noted that the fault plane is simulated by mica powder, with a thickness of 10 mm [14].

3. Result Analysis of Physical Simulation Test

3.1. Structure Evolution of Overlying Strata with Different Mining Directions. Typical mining states of two models are

Table 1: Similarity ratios of the physical model.

Geometric C_l	Time C_t	Density C_ρ	Elastic modulus C_E	Strength C_σ
200	14	1.5	300	300

Table 2: Lithology and physical-mechanical parameters of roof-floor strata [14].

Lithology	Density		Compressive strength		Elastic modulus		Materials ratio
	Prototype (kg·m^{-3})	Model (kg·m^{-3})	Prototype (MPa)	Model (kPa)	Prototype (GPa)	Model (MPa)	
Siltstone	2400	1600	27.60	92.00	4.56	15.20	755
Pack sand	2400	1600	31.50	105.00	5.04	16.80	782
Gritstone	2400	1600	36.00	120.00	4.86	16.20	773
Coal	2400	1600	16.00	53.30	2.34	7.80	864
Mudstone	2250	1500	17.20	57.40	2.94	9.80	864
Sandy mudstone	2250	1500	21.10	70.30	2.94	9.80	864
Silty mudstone	2250	1500	17.20	57.40	2.94	9.80	864

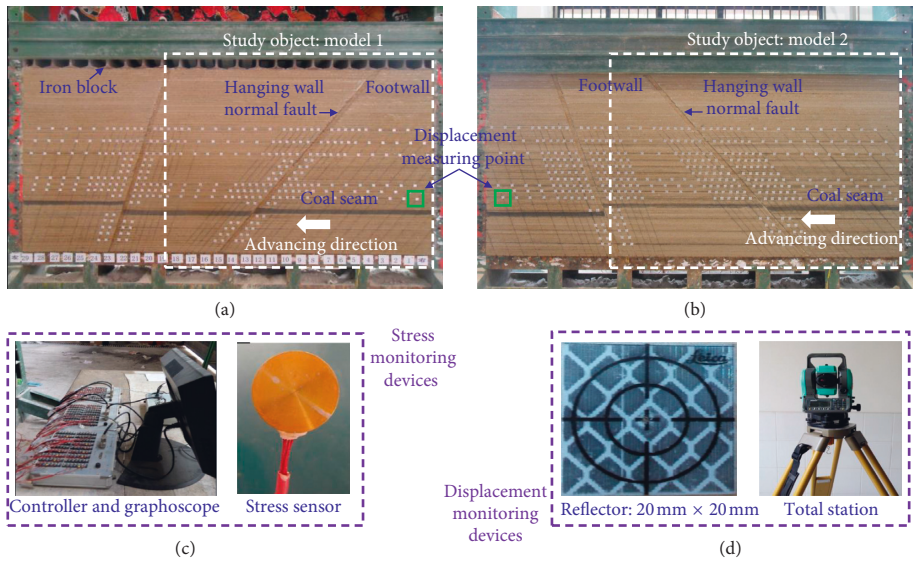

Figure 2: Overview of Model 1 (a) and Model 2 (b). Stress monitoring device (c). Displacement monitoring device (d).

selected to study the structure evolution of overlying strata affected by fault, as shown in Figures 3 and 4.

In Model 1, the mining disturbance has a small effect on the fault with $L_F \geq 40$ m, and the overlying strata structure evolves conventionally, as shown in Figure 3(a). When $40\text{ m} > L_F \geq 0$ m (as shown in Figures 3(b) and 3(c)), the fault begins to affect by mining disturbance and gradually enhances, and the fault is notably activating and slipping; the footwall strata move fully, and the displacement is large. When the face passes through the fault, as in Figures 3(d) and 3(e), the overall movement of the hanging wall is relatively small due to stable invert-wedge-shaped strata structure formation affected by fault dip.

As shown in Figure 4, the overlying structure of Model 2 with $L_H = 60$ m is similar to the one of Model 1, which indicates that the effect of fault dip on strata behaviors is not obvious. When $60\text{ m} > L_H \geq 0$ m, the hanging wall strata are stable and move slightly because of the invert-wedge-shaped structure, and fault activation is not obvious. When the face passes through the fault with $L_H < 0$ m, the footwall strata display a wedge shape and present several times of rotation and cutting collapse, resulting in notable fault slipping.

3.2. Movement of Overlying Strata with Different Mining Directions. The displacement monitoring lines are selected to study the roof displacement variations quantitatively, with different directions as shown in Figure 5. Herein, the monitoring line of Model 1 above the footwall coal seam is 38 m, while that of Model 2 is 32 m.

In Figure 5(a), when $L_F = 40$ m and 30 m, the footwall strata movement is less affected by the fault. Subsequently, the footwall strata move suddenly, and the displacement rises notably due to fault cutting and fault activation, with $L_F = 10$ m. After that, the displacement varies suddenly again because of the hanging wall strata rotation and cutting collapse with $L_F = -30$ m, and then it has no mutation.

In Figure 5(b), the hanging wall strata move slightly, and the displacement has no sudden change, because of the stable invert-wedge-shaped structure of hanging wall strata with L_H

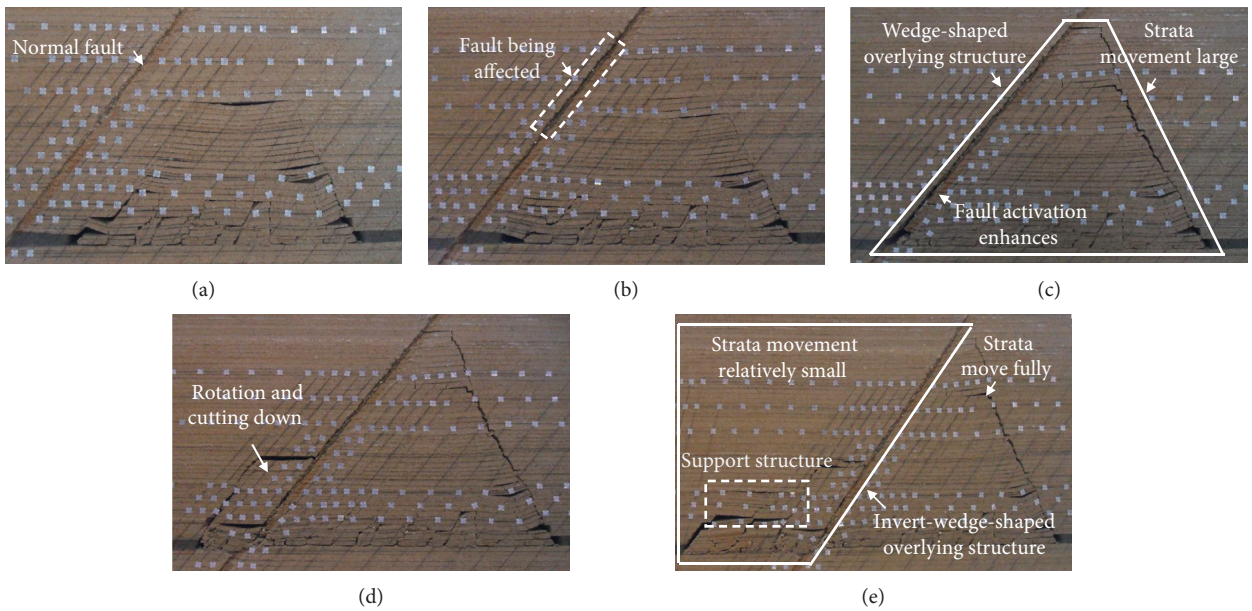

FIGURE 3: Structure evolution of overlying strata with mining from the footwall (Model 1). (a) $L_F = 40$ m. (b) $L_F = 20$ m. (c) $L_F = 0$ m. (d) $L_F = -30$ m. (e) $L_F = -110$ m.

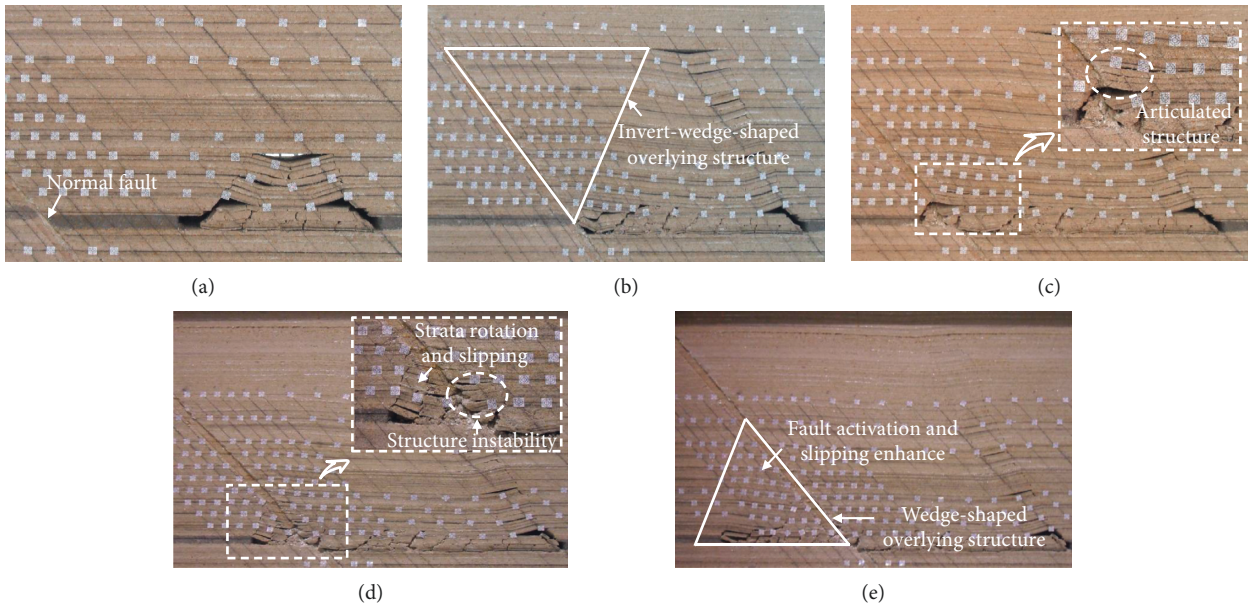

FIGURE 4: Structure evolution of overlying strata with mining from the hanging wall (Model 2). (a) $L_H = 60$ m. (b) $L_H = 0$ m. (c) $L_H = -20$ m. (d) $L_H = -40$ m. (e) $L_H = -100$ m.

≥ -30 m. When $L_H = -40$ m, the footwall strata start rotating and cutting down, resulting in fault slipping, and the displacement rises violently. Subsequently, the mining effect on fault is reduced, and the displacement variation is normal.

Hence, because of fault cutting and fault dip, the movement characteristics of overlying strata with different mining directions are different, and the positions of the displacement mutational point are different, which indicates that the risk area caused by strata sudden movement is different; however, this always occurs during the mining process in the footwall.

3.3. Fault-Slipping Characteristics with Different Mining Directions. The relative displacement of two fault walls can be obtained by recording two points at both sides of fault; then, the fault-slipping characteristics with different mining directions are analyzed as shown in Figure 6.

In Figure 6(a), because of the small mining effect on fault with $L_F \geq 40$ m, the relative displacement of two fault walls is small. When $40\text{ m} > L_F \geq 0$ m, the mining effect on the fault aggravates gradually, and the displacement of the footwall point rapidly rises to 5.2 m, while that of the hanging wall point is small with 1.8 m, resulting in the relative

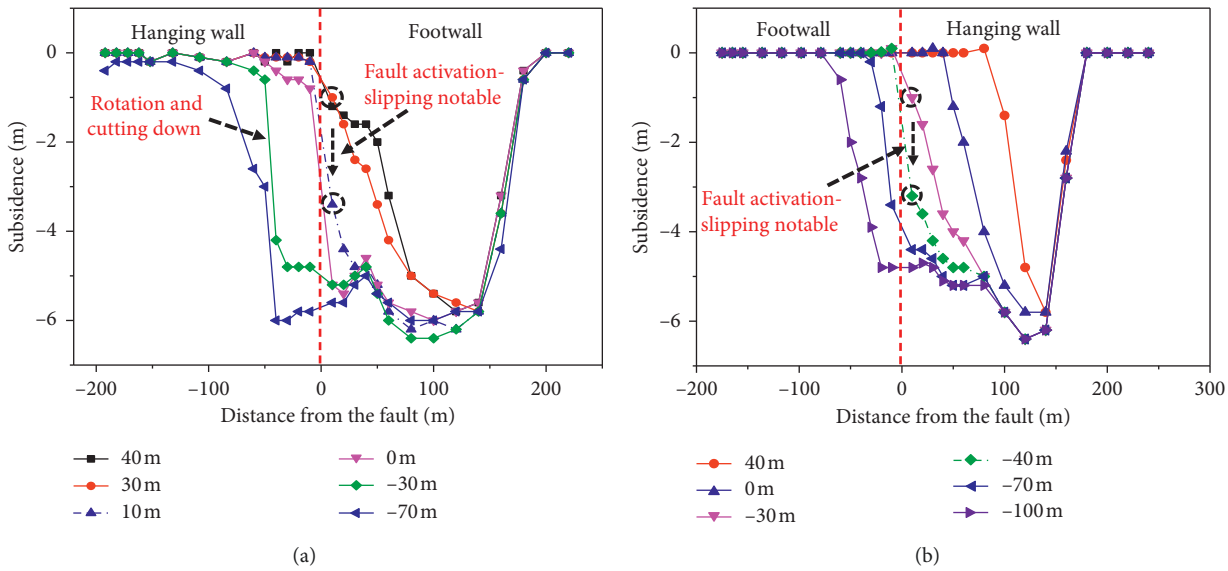

Figure 5: Displacement of overlying strata with different mining directions. (a) Footwall mining. (b) Hanging wall mining.

displacement rising sharply to the peak value of 3.4 m. After that, the footwall strata have been moved fully with $L_H < 0$ m, while the hanging wall point rises violently due to the strata rotation and cutting collapse; therefore, the relative displacement drops notably, and then the mining effect on fault is weakened, and the displacement variation tends to be stable.

In Figure 6(b), prior to passing of the fault with $L_H \geq 0$ m, the relative displacement is 0 m and there is no fault slipping because the fault activation is not prominently caused by the invert-wedge-shaped structure of the hanging wall strata. After the passing of the fault with $L_H < 0$ m, the displacement of the two points rises sharply due to the footwall strata rotation and cutting collapse, resulting in a large relative displacement, and the fault slipping is obvious, and the peak value reaches 3.2 m with $L_H = -60$ m. When $L_H = -90$ m, the strata on two fault walls move slowly and the relative displacement is small.

Hence, based on the aforementioned analysis, the notable fault-affected zone differs with different advancing directions: the footwall face passing through the fault is true for 40 m $> L_F \geq -70$ m, while the hanging wall face passing through the fault exists for -10 m $> L_H \geq -90$ m.

3.4. Abutment Stress of Coal Body with Different Mining Directions. In this section, five sensors at floor strata (S5, S7, S9, S11, and S14) in Model 1 and four sensors (S4, S6, S9, and S11) in Model 2 are chosen to study the abutment stress of the coal body. In Model 1, S5 is at the footwall and far from the fault 30 m, S7 is near the fault and far from the fault 10 m at the footwall, and S9, S11, and S14 are at the hanging wall and far from the fault 20 m, 48 m, and 106 m, respectively. In Model 2, S4 is at the hanging wall and far from the fault 48 m, S6 and S9 are near the fault at both sides within 20 m, and S11 is at the footwall and far from the fault 47 m. Figure 7 depicts the variation curves of abutment stress for the coal body with different mining directions.

As shown in Figure 7(a), in Model 1, the abutment stress peak value of S5 is only 0.08 MPa, with the face far away from the fault and slightly affected by the fault. With the face passing closing to the fault, the stress at S7 rises notably to a peak value of 0.18 MPa, caused by fault activation and slipping. Then, the stress of S9 and S11 increases due to the hanging wall strata rotation and slipping, with just passing through the fault; the stress of S14 continues to rise to a peak value of 0.23 MPa because of the stable strata structure of the hanging wall.

As shown in Figure 7(b), in Model 2, when the working face approaches the fault, the stress rises sharply due to the stable invert-wedge-shaped structure and fault block effect, and the peak value of S6 reaches 0.14 MPa which is 2 times the peak value of S4 (0.07 MPa). When the working face passes through the fault, the abutment stress of S11 increases gradually due to the footwall strata rotation and cutting collapse, which exerts load on the footwall coal seam.

3.5. Fault Plane Stress with Different Mining Directions. When the working face approaches the fault, the fault is affected by the mining activities, resulting in in situ stress on the fault plane variation. Hence, according to the stress monitoring scheme [14], the normal stress variations of the fault plane with different mining directions are studied, in order to analyze the relationship among the mining disturbance, fault plane stress, and the rock burst induction, as shown in Figure 8.

Measurements from two sensors, S23 (vertical distance above the footwall coal seam of 40 m in Model 1) and S24 (vertical distance above the hanging wall coal seam of 20 m in Model 2), placed along the fault plane are depicted in Figure 8. Normal stresses of the fault plane of both models remain unchanged at 0 MPa, when the monitoring position of fault is not affected by mining disturbance. However, when the face approaches the fault in Model 1, the stress of S23 notably rises to the peak value of 0.06 MPa, due to the

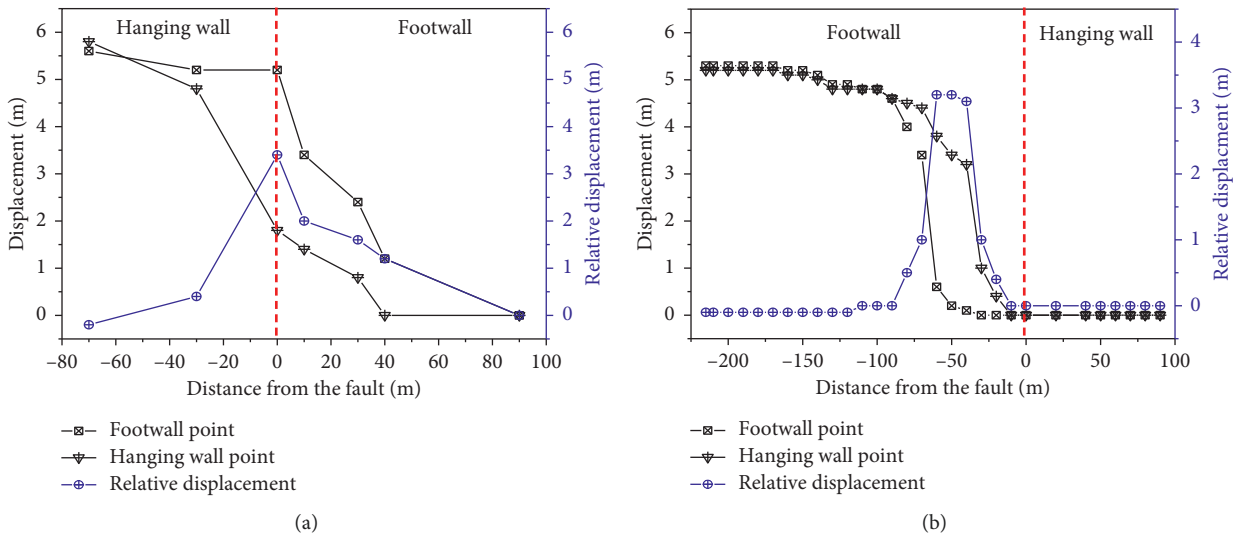

Figure 6: Variation curves of displacement and relative displacement of two fault walls. (a) Footwall mining. (b) Hanging wall mining.

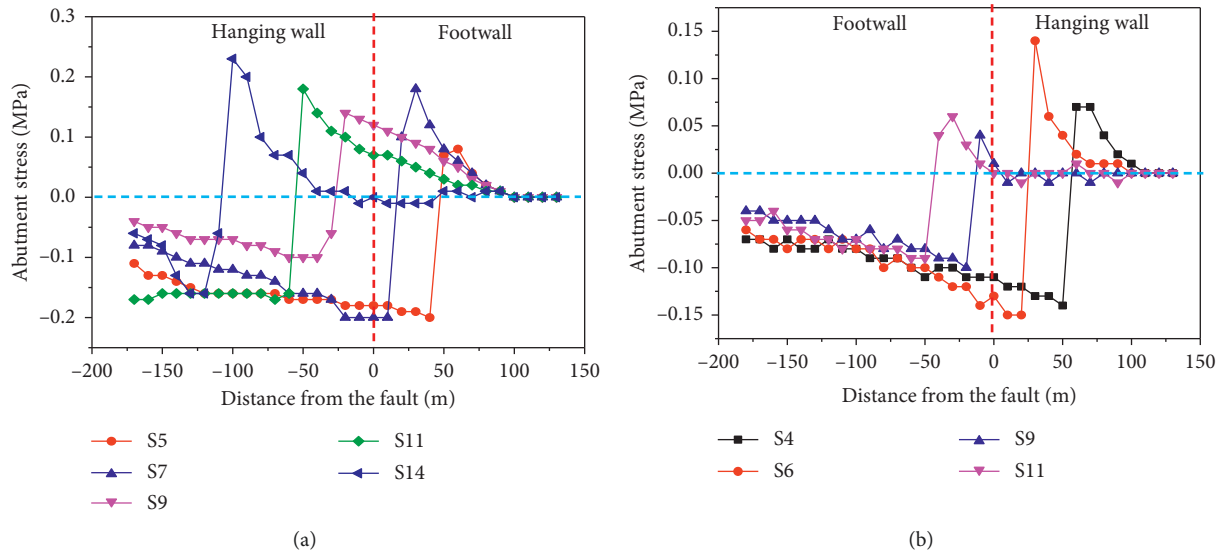

Figure 7: Variation curves of abutment stress for the coal body. (a) Footwall mining. (b) Hanging wall mining.

extrusion and closure of the fault plane caused by the surrounding strata rotation (Figure 3(b)); then, it drops because of the fault plane opening caused by mining disturbance (Figure 3(c)), and the stress dropping stage is fittingly corresponding to the stage of sudden increase in displacement as shown in Figures 5(a) and 6(a). In Model 2, the normal stress rises suddenly to a peak value of 0.05 MPa after the face just passes the fault because of an articulated structure formation (Figure 4(c)) and bearing the large horizontal force, and it drops sharply to −0.04 MPa due to articulated structure instability (Figure 4(d)); this stage is also fittingly corresponding to the stage of sudden increase in displacement as shown in Figure 6(b).

Therefore, regardless of the mining direction in both physical models, the normal stress dropping stage is exactly corresponding to the stage of sudden increase in displacement, which indicates that the mining disturbance causes the in situ stress variation of the fault plane, and then the fault activates and slips suddenly, thereby resulting in the risk of fault rock burst. In addition, due to the different mining directions, the causes of stress variation of the fault plane are also different, which can conduct to the control surrounding rocks near the fault.

3.6. Influence of Different Advancing Directions on Mining Effect Caused by a Fault. From the aforementioned analysis, for the footwall face prior to passing the fault (Model 1), the footwall strata present a wedge-shaped structure with poor stability in the fault-affected zone. Moreover, the effect of fault activation is enhanced gradually, and the fault slipping is notable, which leads to the variation of fault plane stress and the rise of abutment stress of the footwall coal body; the footwall strata move fully, and the displacement is large.

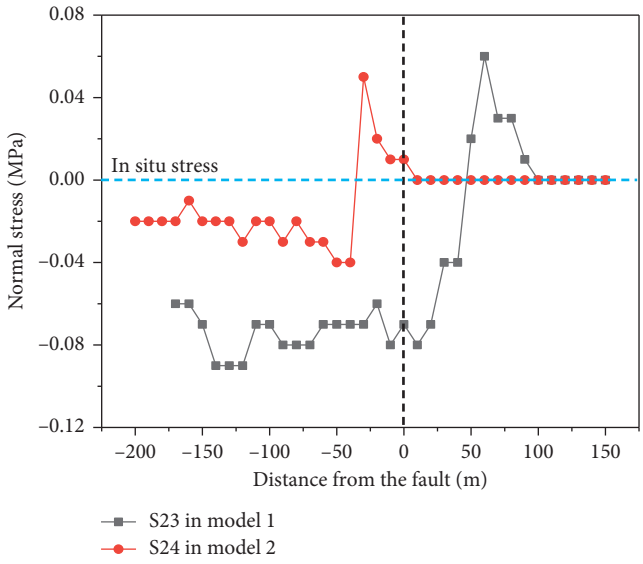

Figure 8: Variation curves of normal stress for the fault plane.

After passing through the fault, the hanging wall strata form an invert-wedge-shaped structure with good stability, resulting in the rise of abutment stress of the coal body in the hanging wall; moreover, the effect of fault activation weakens gradually, and the displacement of the hanging wall is relatively small compared with that of the footwall.

For the hanging wall face prior to passing the fault (Model 2), the invert-wedge-shaped overlying structure of the hanging wall is stable in the fault-affected zone, resulting in unobvious fault activation and in the rise of abutment stress of the coal body in the hanging wall. After passing through the fault, fault activation and slipping are notable due to the footwall strata rotation and subsidence which leads to the articulated structure instability and the rise of abutment stress of the footwall coal body.

Hence, it can be concluded that the overlying structure varies notably, affected by fault cutting and fault dip, and the fault-affected zone and the cause of rock burst induction with different mining directions are different. However, regardless of the mining direction, the overlying structure of the hanging wall is stable and the fault activation is not obvious, while that of the footwall is relatively active and the fault activation there is violent. Hence, the risk of rock burst caused on the footwall is larger than that on the hanging wall.

4. Verification of Mining Effect with Different Mining Directions

According to the aforementioned simulation analysis, the mining effect and the fault activation when the footwall face is mined are more notable. Hence, based on the relationship between the mining direction and the fault dip, two mechanical models of roof rock in the fault-affected zone are simplified in order to verify the above simulation results. Figure 9 depicts the mechanical analysis of roof rock near fault with different mining directions.

In Figure 9, the roof block marked as A is used as the study object, and a mechanical analysis is conducted. By using equilibrium conditions, the normal force F_σ and friction force F_f of the fault plane can be expressed as follows.

Footwall mining:

$$\begin{cases} F_\sigma = T\sin\alpha + R\cos\alpha, \\ F_f = T\cos\alpha - R\sin\alpha. \end{cases} \quad (1)$$

Hanging wall mining:

$$\begin{cases} F_\sigma = T\sin\alpha - R\cos\alpha, \\ F_f = -T\cos\alpha - R\sin\alpha, \end{cases} \quad (2)$$

where $R = f_\mu + pL + P - ql - G$.

From equations (1) and (2), it can be seen that when the working face approaches the fault, the support performance of the coal pillar for overlying strata decreases, which results in the drop of the value of parameter R. If the variation of horizontal force T in Figure 9 can be ignored, the normal force F_σ of the fault plane will decrease and the friction force F_f of the fault plane will increase when the footwall face advances towards fault, resulting in the rise of the ratio of the shear stress to the normal stress of the fault plane; this indicates that the mining effect on fault activation and slipping is notable, and the block A can easily slip along the fault plane, rendering the formation of a stable structure difficult. Meanwhile, the normal force F_σ of the fault plane will increase and the friction force F_f of the fault plane will decrease when the hanging wall face advances towards fault, and the ratio of the shear stress to the normal stress of the fault plane drops; this indicates that the fault activation is not obvious, and the rocks can easily form a stable structure. Hence, the mining direction has a significant influence on the mining effect with a fault occurrence; that is, compared with the hanging wall mining, the mining effect caused by fault is notable, and dynamic appearance is more serious when the face is mined in the footwall, which verifies some aforementioned simulation results.

5. Engineering Case of Rock Burst with Footwall Mining

From the above numerical simulation and theoretical analysis, the fault risk is closely related to the position relationship between fault and working face, as well as the mining direction of the face. However, in both Model 1 and Model 2 in the simulation tests, when the working face is being mined in the hanging wall, the overlying structure is stable and the fault activation is not obvious, while that of footwall mining is relatively active and the fault activation there is violent; hence, the risk of rock burst with footwall mining is larger than that of mining on the hanging wall. Therefore, in this section, an engineering case occurring in the Baodian coal mine is chosen, in order to study the rock burst easily induced with footwall mining and further more to verify some aforementioned results.

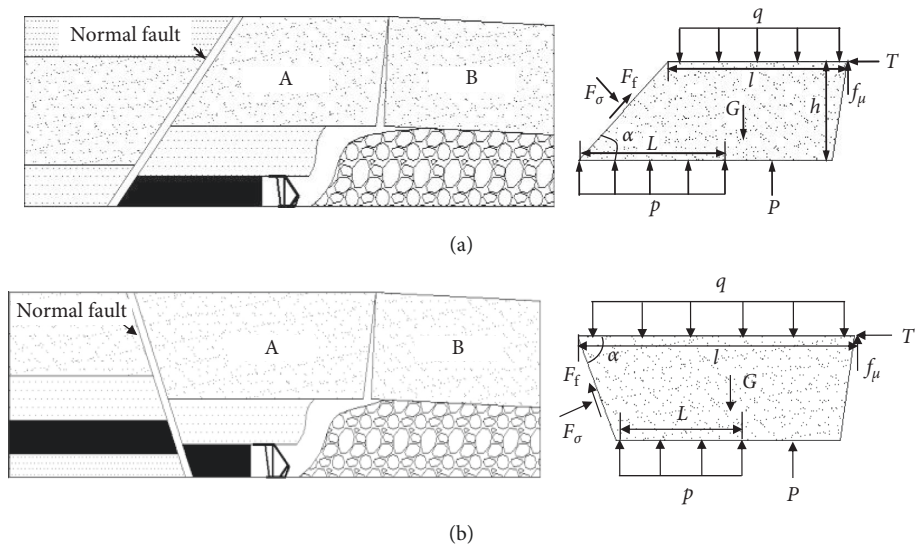

Figure 9: Mechanical analysis of roof rock near fault with different mining directions. (a) Footwall mining. (b) Hanging wall mining.

The mining depth of panel 6303 is 680 m–700 m, and the average coal seam thickness is 4.75 m which has the strong bursting liability. When the distance between the working face (indicates the side of the tailgate) and the normal fault (SF28: $\angle 47^\circ$ $H = 3$ m; H represents the fault fall height) is 52 m, as on November 30, 2004, a rock burst accident occurs in the tailgate 66 m–96 m ahead of the coal wall; another rock burst accident occurs in the tailgate 12 m–36 m ahead of the coal wall, when the working face is away from the fault 24 m, as on December 16, 2004. Figure 10 shows the positions of the working face and the accidents [24].

According to the geological report of panel 6303, both rock burst accidents occur during the mining in the footwall of SF28, and they are affected by the fault notably. Herein, a small fault coal pillar with a width of 10 m is formed in the headgate side when the accident occurs at the tailgate, as on November 30, 2004, while another accident on December 16, 2004, also occurred in the tailgate with a coal pillar of 24 m at the tailgate side. From the cause analysis of the accidents for the geological report, it is deduced that coal pillars with the width of 10 m and 24 m are small due to the fault cutting, and fault activates notably affected by mining operations and fault dip, resulting in the fault easily slipping and the high stress concentrating in the coal body, eventually leading to the two rock burst accidents in the tailgate with the sudden release of strain energy. This is similar to the aforementioned analysis of the results of a similar model test; that is, when the working face in the footwall approaches the fault, the footwall strata form a wedge-shaped structure with poor stability, and the fault activation and slipping are notable (as shown in Figures 3(c) and 6(a)); this leads to the footwall strata moving suddenly and causes the abutment stress of coal body to rise, as shown in Figures 5(a) and 7(a). Hence, to a certain extent, the case engineering can be used to verify some study results of physical simulation tests of this paper and can further explain the rationality of the similar simulation method.

6. Conclusions

In this study, two physical models, utilizing similar materials, are established, and the influence of advancing directions on mining effect caused by a fault is studied; moreover, rock bursts affected by fault with different mining directions are compared and analyzed. We can obtain several conclusions as follows:

(i) For the footwall face prior to passing the fault (Model 1), the footwall overlying structure presents a wedge shape and has poor stability in the fault-affected zone; moreover, the effect of fault activation is enhanced gradually, and fault slipping is notable, which leads to the variation of fault plane stress and the rise of abutment stress of the footwall coal body; the footwall strata move fully, and the displacement is large. After passing through the fault, the hanging wall strata form an invert-wedge-shaped structure with good stability, resulting in the rise of abutment stress of the coal body in the hanging wall; moreover, the effect of fault activation weakens gradually, and the displacement in the hanging wall is relatively small compared with that in the footwall.

(ii) For the hanging wall face prior to passing the fault (Model 2), the invert-wedge-shaped overlying structure of the hanging wall is stable in the fault-affected zone, resulting in an unobvious fault activation and a rising abutment stress of the coal body in the hanging wall. After passing through the fault, fault activation and slipping are notable due to the footwall strata rotation and subsidence, which leads to articulated structure instability and a rising abutment stress of the footwall coal body.

(iii) The overlying structure varies, notably affected by fault cutting and fault dip, and the fault-affected zone differs with different mining directions. The

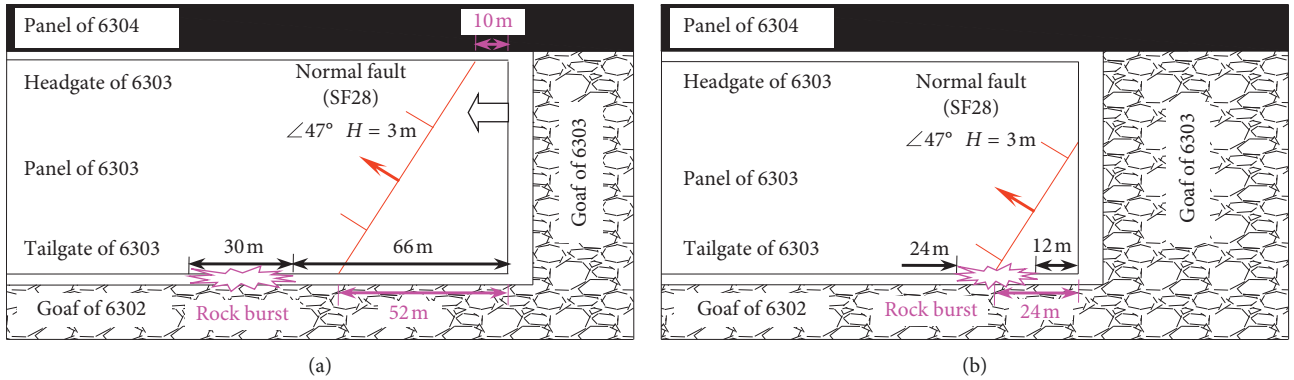

Figure 10: Rock burst accidents of panel 6303.

hanging wall structure is stable and the fault activation is unobvious, while that of the footwall is relatively active and the fault activation there is violent. Hence, the risk of rock burst on the footwall is larger than that of mining on the hanging wall.

Finally, an engineering case regarding two rock bursts in panel 6303 is used to verify several simulation results to a certain extent.

The study results can serve as a reference for predicting and preventing rock bursts under similar conditions and can optimize the layout for the working face near the fault.

Abbreviations

C_l: Geometric similarity ratio
C_ρ: Density similarity ratio
C_σ: Strength similarity ratio
C_E: Elastic modulus similarity ratio
C_t: Time similarity ratio
l_m: Geometric size of the physical model (m)
l_p: Geometric size of the prototype (m)
ρ_m: Densities of the physical model (kg/m^3)
ρ_r: Densities of the prototype (kg/m^3)
L: Distance between the working face and the objected fault (m)
L_F: Distance between the working face in the footwall and the objected fault of Model 1 (m)
L_H: Distance between the working face in the hanging wall and the objected fault of Model 2 (m)
q: Overlying uniform load (N/m)
p: Uniform load supported by the coal body (N/m)
G: Deadweight of block A (N)
T: Horizontal force exerted by block B (N)
A: Block number near the fault
B: Block number articulated with block A
f_μ: Friction force between blocks A and B (N)
P: Support power of the hydraulic support (N)
F_σ: Normal force exerted by the other wall rocks (N)
F_f: Friction force between two fault walls (N)
R: Constant related to the parameters f_μ, p, L, P, q, l, and G
α: Fault dip angle (°)
l: Length of the uniformly distributed load (m)
h: Height of block A.

Data Availability

The data used to support the findings of this study are available from the corresponding author upon request.

Conflicts of Interest

The authors declare that there are no conflicts of interest regarding the publication of this paper.

Acknowledgments

The study was supported by the National Key R&D Program of China (2018YFC0604703), SDUST Research Fund, National Natural Science Foundation of China (nos. 51574155, 51704182, 51804182, and 51504145), Natural Science Foundation of Shandong Province (no. ZR2017BEE050), Science and Technology Development Plan of Tai'an (2018GX0045), and Scientific Research Foundation of Shandong University of Science and Technology for Recruited Talents (no. 2015RCJJ057).

References

[1] S. Zhu, Y. Feng, F. Jiang, and J. Liu, "Mechanism and risk assessment of overall-instability-induced rockbursts in deep island longwall panels," *International Journal of Rock Mechanics and Mining Sciences*, vol. 106, pp. 342–349, 2018.

[2] Y. Yong, T. Shihao, Z. Xiaogang, and L. Bo, "Dynamic effect and control of key strata break of immediate roof in fully mechanized mining with large mining height," *Shock and Vibration*, vol. 2015, Article ID 657818, 11 pages, 2015.

[3] C. Fan, S. Li, M. Luo, W. Du, and Z. Yang, "Coal and gas outburst dynamic system," *International Journal of Mining Science and Technology*, vol. 27, no. 1, pp. 49–55, 2017.

[4] P. Wang, L. S. Jiang, J. Q. Jiang, P. Q. Zheng, and W. Li, "Strata behaviors and rock-burst-inducing mechanism under the coupling effect of a hard thick stratum and a normal fault," *International Journal of Geomechanics*, vol. 18, no. 2, article 04017135, 2018.

[5] C. Mark, "Coal bursts that occur during development: a rock mechanics enigma," *International Journal of Mining Science and Technology*, vol. 28, no. 1, pp. 35–42, 2018.

[6] L. Jiang, P. Wang, P. Zhang, P. Zheng, and B. Xu, "Numerical analysis of the effects induced by normal faults and dip angles

on rock bursts," *Comptes Rendus Mécanique*, vol. 345, no. 10, pp. 690–705, 2017.

[7] H. G. Ji, H. S. Ma, J. A. Wang, Y. H. Zhang, and H. Cao, "Mining disturbance effect and mining arrangements analysis of near-fault mining in high tectonic stress region," *Safety Science*, vol. 50, no. 4, pp. 649–654, 2012.

[8] Y. D. Jiang, T. Wang, Y. X. Zhao, and C. Wang, "Numerical simulation of fault activation pattern induced by coal extraction," *Journal of China University of Mining and Technology*, vol. 42, no. 1, pp. 1–5, 2013.

[9] S. A. Bornyakov, I. A. Panteleev, and A. A. Tarasova, "Dynamics of intrafault deformation waves: results of physical simulation," *Doklady Earth Sciences*, vol. 471, no. 2, pp. 1316–1318, 2017.

[10] A. Sainoki and H. S. Mitri, "Dynamic behaviour of mining-induced fault slip," *International Journal of Rock Mechanics and Mining Sciences*, vol. 66, no. 1, pp. 19–29, 2014.

[11] J. Q. Jiang, Q. L. Wu, and H. Qu, "Characteristic of mining stress evolution and activation of the reverse fault below the hard-thick strata," *Journal of China Coal Society*, vol. 40, no. 2, pp. 267–277, 2015.

[12] F. X. Jiang, Q. D. Wei, C. W. Wang et al., "Analysis of rock burst mechanism in extra-thick coal seam controlled by huge thick conglomerate and thrust fault," *Journal of China Coal Society*, vol. 39, no. 7, pp. 1191–1196, 2014.

[13] N. B. Zhang, Z. H. Ouyang, S. K. Zhao, H. Y. Li, and Z. G. Deng, "Research on the occurrence mechanism of fault rock-burst based on the stick-slip theory," *Chinese Journal of Underground Space and Engineering*, vol. 12, no. 2, pp. 874–898, 2016.

[14] P. Wang, L. S. Jiang, and P. Q. Zheng, "Application of equivalent materials to modeling fractures in the vicinity of a normal fault in the area of mining exploitation influence," *Acta Geodynamica et Geomaterialia*, vol. 14, no. 4, pp. 475–485, 2017.

[15] J.-b. Peng, L.-w. Chen, Q.-b. Huang, Y.-m. Men, W. Fan, and J.-k. Yan, "Physical simulation of ground fissures triggered by underground fault activity," *Engineering Geology*, vol. 155, no. 2, pp. 19–30, 2013.

[16] Y. K. Liu, F. B. Zhou, L. Liu, C. Liu, and S. Y. Hu, "An experimental and numerical investigation on the deformation of overlying coal seams above doubleseam extraction for controlling coal mine methane emissions," *International Journal of Coal Geology*, vol. 87, no. 3-4, pp. 139–149, 2011.

[17] S. C. Zhang, W. J. Guo, W. B. Sun, Y. Y. Li, and H. L. Wang, "Experimental Research on extended activation and water inrush of concealed structure in deep mining," *Rock and Soil Mechanics*, vol. 36, no. 11, pp. 3111–3120, 2015.

[18] S. Zhang, W. Guo, Y. Li, W. Sun, and D. Yin, "Experimental simulation of fault water inrush channel evolution in a coal mine floor," *Mine Water and the Environment*, vol. 36, no. 3, pp. 443–451, 2017.

[19] H. Y. Dai, X. G. Lian, J. Y. Liu et al., "Model study of deformation induced by fully mechanized caving below a thick loess layer," *International Journal of Rock Mechanics and Mining Sciences*, vol. 47, no. 6, pp. 1027–1033, 2010.

[20] H. C. Li, *Similar Simulation Test for Ground Pressure*, China University of Mining and Technology Press, Xuzhou, China, 1988.

[21] C. Wang, N. Zhang, Y. Han, Z. Xiong, and D. Qian, "Experiment Research on overburden mining-induced fracture evolution and its fractal characteristics in ascending mining," *Arabian Journal of Geosciences*, vol. 8, no. 1, pp. 13–21, 2013.

[22] X. P. Lai, P. F. Shan, J. T. Cao, F. Cui, and H. Sun, "Simulation of asymmetric destabilization of mine-void rock masses using a large 3D physical model," *Rock Mechanics and Rock Engineering*, vol. 49, no. 2, pp. 487–502, 2015.

[23] J. Xie, W. Zhu, J. Xu, J. Wen, and C. Liu, "A study on the bearing effect of pier column backfilling in the goaf of a thin coal seam," *Geosciences Journal*, vol. 20, no. 3, pp. 361–369, 2015.

[24] Z. H. Li, *Research on rock burst mechanism induced by fault slip during coal mining operation*, Ph.D. Dissertation, China University of Mining and Technology, Xuzhou, China, 2009.